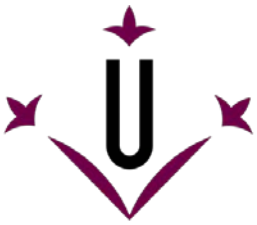

Quarantining the Sahara desert: Growth and water–use efficiency of Aleppo pine in the Algerian Green Barrier

Zineb Choury[1], Tatiana A. Shestakova[2], Hocine Himrane[3], Ramzi Touchan[4], Dalila Kherchouche[5], J. Julio Camarero[6], Jordi Voltas[1*]

[1]Department of Crop and Forest Sciences – AGROTECNIO Center, University of Lleida, E–25198 Lleida, Spain

[2]Department of Ecology, University of Barcelona, E–08028 Barcelona, Spain

[3]Institute National de Recherche Forestière, Arboretum de Bainem, B.P. 37 Cheraga, Algeria

[4]Laboratory of Tree Ring Research, The University of Arizona, Tucson, AZ 85721, USA

[5]Institute of Veterinary and Agronomy Sciences, The University Hadj-Lakhdar, Batna 05000, Algeria

[6]Pyrenean Institute of Ecology, IPE–CSIC, E–50059 Zaragoza, Spain

*Corresponding Author:

Jordi Voltas

Department of Crop and Forest Sciences – AGROTECNIO Center University of Lleida.

Alcalde Rovira Roure 191, E–25198 Lleida, Spain

tel. +34 973 702855; e–mail: jvoltas@pvcf.udl.cat

Acknowledgements

We acknowledge the support of the International Atomic Energy Agency (project ALG5028) to H. Himrane and of the Spanish project FUTURPIN (AGL2015–68274–C3–3–R) to J. Voltas. We also acknowledge funding provided by the US National Science Foundation, Earth System History (Award No. 0317288) and Paleo Perspectives on Climate Change (Award No. 1103314). An earlier version of this work was presented by Z. Choury to obtain a MSc degree in the Erasmus Mundus Programme MEDfOR. T.A. Shestakova is supported by ERANET–Mundus (European Commission). We remain indebted to P. Sopeña and M.J. Pau for technical assistance.

Abstract

The Algerian Green Barrier, mainly composed of native and artificial Aleppo pine forests, spreads along the presaharian steppes and is threatened by anthropogenic and natural disturbances, including climate change. We hypothesized that the ecophysiological functioning of this conifer has been substantially modified in reaction to recent warming and drought much beyond the expected effect of CO_2 fertilization. Our aim was to characterize the long-term performance (1925-2013) of native Aleppo pines thriving at their southernmost distribution. We used tree-ring width (TRW) and carbon isotope discrimination ($\Delta^{13}C$) to characterize basal area increment (BAI) and water-use efficiency (WUEi) at three sites. BAI remained stable or slightly increased over time, with mean values ranging between 4.0 and 6.3 cm^2 $year^{-1}$. Conversely, site–$\Delta^{13}C$ decreased from –0.022 to –0.014 ‰ $year^{-1}$ along time, which translated into WUEi increases of *ca*. 39%. This strong physiological reaction indicates that pines are responding simultaneously to rising CO_2 and drier conditions, inducing a progressively tighter stomatal control of water losses. However, WUEi increments were essentially unrelated to BAI and did not affect carbon reserves, which suggests a high resilience to climate change. This finding could be due to shifts in growing season towards earlier months in winter-spring, as suggested by temporal changes in climate factors underlying $\Delta^{13}C$ and TRW. Our study highlights the substantial plasticity of Aleppo pine, but this species is unlikely to follow a similar pace of ecophysiological adjustments according to unprecedented low $\Delta^{13}C$ records and lack of WUEi stimulation observed from 2000 onwards.

Keywords: carbon isotope discrimination; dendroecology; forest growth; water–use efficiency; Maghreb; *Pinus halepensis*

Introduction

The Mediterranean Basin is an important biodiversity hotspot and an important geo–strategic region that is very sensitive to the impact of climate change (Thuiller et al. 2005), and particularly so in the case of the North African countries (Giorgi and Lionello, 2008). For example, there is evidence of strong drying over large portions of the Maghreb and these drought patterns seem to be linked to the warming of the Indian Ocean waters (Hoerling et al. 2012). Some recent reconstructions of the circum–Mediterranean drought variability indicate that the late 20th century was among the driest periods in Northwest Africa for the past 900 years (Touchan et al. 2008; Touchan et al. 2011; Cook et al. 2016). If the climate becomes warmer and drier, regional forest growth and adaptation may be severely affected, threatening terrestrial ecosystems of extraordinary environmental and social value.

The Algerian forests occupy three main geographical areas in the country's wetter north, where climate conditions are more favourable for tree growth: the Tellian Atlas, running in parallel to the coast, the Saharan Atlas, marking the northern edge of the Sahara desert, and the zone of the High–Plains that separate them. Although the total Algerian forests account for only 2% of the country's land, they constitute the major ecological barrier that protects from the advance of the Sahara desert (EFI, 2009). In the early 1970s the reforestation project known as 'Green Barrier' was launched to prevent the northward spread of the Sahara, being the most ambitious agro–ecological venture after Algeria's independence in 1962. These reforestations spread over 30,000 km^2 and occupy 123,000 ha along the steppes of the presaharian region, and they were aimed to expand existing native pinewoods as a way to protect against desertification by creating a true barrier of greenness from the Moroccan to the Tunisian borders (Benalia, 2009). However, this Algerian Green Barrier ("*green dam"*) is strongly threatened by

both anthropogenic (overexploitation, grazing) and natural disturbances (forest fires, pest outbreaks), including climate warming (Benalia, 2009).

Pines are the major conifer species of the Mediterranean Basin, where they play keystone ecological and socioeconomical roles (Barbéro et al. 1998). Most pines are isohydric species, able to reduce stomatal conductance during low water availability periods, hence reducing carbon uptake but maintaining relatively constant leaf water potentials regardless of drought intensity (McDowell et al. 2008). The circum–Mediterranean Aleppo pine (*Pinus halepensis* Mill.) is a very plastic species that exemplifies perfectly such general performance (Schiller, 2000; Klein et al. 2014). Its high phenotypic plasticity has been demonstrated for traits such as reproductive efficiency (Santos del Blanco et al. 2013), water uptake patterns (Voltas et al. 2015), radial growth and wood anatomy (De Luis et al. 2013; Pacheco et al. 2016) or water–use efficiency (Ferrio et al. 2003).

Long–term annual records of radial growth and water–use efficiency are common for high–elevation Mediterranean pine forests where tree performance depends chiefly on temperature variations and does not always reflect drought variability (e.g. Galván et al. 2015). However, dendrochronological studies are rare in North Africa forests (e.g. Touchan et al. 2011; Touchan et al. 2016), except for mountain Moroccan cedars (Atlas and Rif), which have been systematically surveyed since the 1970s (e.g. Munaut, 1978; Berger et al. 1979; Till and Guiot, 1990; Chbouki et al. 1995; Esper et al. 2007). The main reason of this deficiency is the difficulty, in many cases, to identify and date annual rings unequivocally (Cherubini et al. 2003). Moreover, in Mediterranean regions the cambial activity stops in winter under low temperatures, but also in peak summer, coincident with the period of maximum drought stress, which leads to bimodal growth patterns (Camarero et al. 2010). This ‘double–stress’

(Mitrakos, 1980) may induce the formation of false or double rings characterized by intra–annual density fluctuations (De Luis et al. 2011), and also the occurrence of missing rings (Novak et al. 2016). Despite such impediments, a tree–ring chronology of *Pinus halepensis* from north-western Tunisia, for example, allowed reconstructing precipitation patterns spanning the last 230 years, which represents a valuable tool for long–term water resources planning (Touchan et al. 2008). If tree–ring–based studies are scarce for the Maghreb, they are just non–existent (to the best of our knowledge) for stable isotopes, which are nowadays widely used to gain information on leaf–level physiological responses to environmental factors (McCarroll and Loader, 2004; Gessler et al. 2014). Changes in gas exchange are recorded in annual rings through carbon isotope discrimination ($\Delta^{13}C$), which gives insight into how trees respond to drought (e.g., Saurer et al. 2014; Shestakova et al. 2014). Particularly, the ratio of the heavy to light carbon isotopes ($^{13}C/^{12}C$ or $\delta^{13}C$) depends on factors affecting CO_2 uptake, being mainly controlled by photosynthetic rate (A) and stomatal conductance (g_s), as expressed in the ratio A/g_s (intrinsic water–use efficiency, WUEi; Farquhar et al. 1989).

Here we aim at identifying the climatic factors driving tree performance of native Aleppo pine forests over the last 90 years in the Algerian Saharan Atlas, an area characterized by an arid bioclimate with large diurnal and seasonal thermal variations. We hypothesize that the ecophysiological performance of a highly plastic species such as Aleppo pine has been substantially modified at its southernmost distribution range as a reaction to recent warming and drying trends, hence boosting WUEi much beyond what would be expected due to a CO_2 fertilization effect on gas exchange processes. To this end, we pose the following research questions: i) what is the change in tree–ring $\Delta^{13}C$ (a surrogate for WUEi) over the last 90 years (1925–2013 period) and how is it related to radial growth and concurrent carbon storage (i.e. non-structural

carbohydrates)? ii) how tree growth and WUEi are affected by climate factors?; and iii) what is the expected performance of Aleppo pine forests in the near future in the region?

Material and methods

Study area and field sampling

The study was conducted in the high–mountain natural forest area of Sénalba Chergui, Saharan Atlas, Djelfa province, Algeria (Fig. 1). The area is characterized by a continental Mediterranean climate with cold winters and prolonged summer droughts (Fig. 1). The mean annual temperature (MAT) is 14.6ºC, with January being the coldest (5.0ºC) and July the warmest (25.8ºC) month. The mean annual precipitation (MAP) is 360 mm (period 1925–2013), with summer being the driest period of the year accounting for *ca*. 11% of total precipitation (CRU TS3.22 database; Harris et al. 2014) (Fig. 1).

Field sampling was done in summer 2014. Three open stands of Aleppo pine (*Pinus halepensis* Mill.) with density of ~ 150 trees ha^{-1} were selected in a Plateau area (Toughersan), a South–facing slope (Theniat Enser South) and a North–facing slope (Theniat Enser North) of the main ridge of Ouled Naïl mountain (1350 ma.s.l.) (Table 1; Fig. A1). These stands are representative of the biogeographic conditions for natural mountain forests in the green barrier of Algeria, where Aleppo pine is the dominant tree species, with *Quercus ilex* L. and *Juniperus oxycedrus* L. being also present. The mean distance between stands was 8.2 km (± 4.1 km; SD). Two cores per tree from 15 healthy dominant trees per site were sampled at breast height (1.30 m) using a 5–mm Pressler increment borer. For each selected tree, the two increment cores were extracted along

the trunk within a vertical distance of about 5 cm. A total of 87 trees were collected (Table 1).

Sample preparation and dendrochronological methods

Wood samples were air–dried and the surface of one core per tree was sanded with sandpaper of progressively smaller grain to obtain a smooth cross–section. The remaining core per tree was kept intact for carbon isotopes analysis. Tree rings were visually cross–dated and measured with precision of 0.01 mm using a binocular microscope coupled to a computer with the LINTAB package (Rinntech, Heidelberg, Germany). The COFECHA program (Holmes, 1983) was used to evaluate the quality of cross–dating and measurement accuracy of the tree–ring series. Poor samples failing to pass the cross–dating check (presumably due to absent or false rings) were excluded from the process of chronology development (four series of the Plateau site, three series of the North slope and ten series of the South slope). Altogether, 70 trees were finally used for tree-ring width measurements (11, 12, and 47 trees respectively in Plateau, North and South site). To remove long–term trends, each time series of ring–width measurements was detrended individually using a cubic smoothing spline with a 50% frequency cut–off of 67 years (high–pass filtering; Cook and Peters, 1981). This procedure mainly eliminates non–climatic fluctuations, reducing the growth variations that are not common to most trees as well as the effects of stand dynamics. Additionally, an autoregressive model was applied to each detrended series to remove the temporal autocorrelation related to the previous year growth. Finally, a biweight robust mean was used to obtain site tree–ring width (TRW) chronologies consisting of stationary (mean = 1) dimensionless indices. Chronology development and standardization were carried out using the ARSTAN program (Cook and Krusic, 2005).

The quality of the resulting site chronologies was evaluated by calculation of the mean inter–series correlation (*Rbar*), the signal–to–noise ratio (*SNR*) and the Expressed Population Signal (*EPS*) statistics. *Rbar* and *SNR* inform on the strength of the common signal (or common variance) captured by a chronology, with higher values indicating enhanced common signal in both cases (Wigley et al. 1984). *EPS* indicates the suitability of a chronology for capturing the hypothetical population signal, which is usually checked against a threshold value of 0.85 (Wigley et al. 1984). Although the reliable time span for each site chronology comprised at least most of the 20th century (Table 1), we decided to combine all ring-width series from the three sites into a more robust regional chronology owing to the relatively low number of trees available at the Plateau and North sites. The regional chronology reached the EPS threshold value of 0.85 by the mid-19th century (Table 1), therefore allowing for the analysis of climate–growth relationships starting from 1925, in concert with the availability of reliable instrumental records (CRU TS3.22 database; Harris et al. 2014). The regional chronology was checked against a nearby master chronology from the Djelfa region (Touchan et al. 2011). The analysis indicated a good match between both chronologies (Fig. A2).

The annual basal area increment (BAI) was used for characterizing absolute radial growth trends for the set of cross–dated trees at each site. BAI was calculated from tree–ring series according to:

$$BAI = \pi(R_t^2 - R_{t-1}^2) \quad (1)$$

where R is the radius of the tree and t is the year of tree–ring formation.

Carbon isotopes analysis

The carbon isotopes analysis was performed on core segments spanning the period 1925–2013 to avoid a possible juvenile imprint on the isotope values (average age of sampled trees was 125 ± 25 years; mean ± SD). Individual tree rings from five trees per site were identified with the aid of a wet soft brush and excised using a scalpel. For this purpose, the best five cross–dating trees per site were used in order to maximize the isotopic signal common to the sampled trees while keeping the workload of sample processing under reasonable limits. Rings from these five trees were pooled together on an annual basis for isotopic analysis (Leavitt, 2008). In addition, we selected five particular years (1940, 1951, 1971, 1983 and 1999) with contrasting radial growth (wide or narrow rings) in which the individual rings were analysed separately to have an estimate of inter–tree variability of the isotopic signal. The set of rings of the same year and site were milled together to a fine powder with a mixer mill (Retsch MM301, Haan, Germany), except those rings that were analysed independently, which were milled alone. An aliquot of 0.9–1.1 mg of grinded wood was weighed and encapsulated into tin capsules for mass spectrometry analysis. As an alternative to α-cellulose extraction, whole-ring isotope analysis of Aleppo pine has been shown to estimate consistently interannual variability in climate factors (Ferrio and Voltas, 2005). Samples underwent combustion using a Flash EA–1112 elemental analyser interfaced with a Finnigan MAT Delta C isotope ratio mass spectrometer (Thermo Fisher Scientific Inc., MA, USA). The carbon isotope ratios ($^{13}C/^{12}C$) were expressed as carbon isotope composition ($\delta^{13}C$) as follows:

$$\delta^{13}C\,(‰) = \left[\left(R_{sample} / R_{standard}\right) - 1\right] \times 1000 \qquad (2)$$

where R is the isotope (abundance) ratio ($^{13}C/^{12}C$) of the sample (R_{sample}) or of the Vienna Pee Dee Belemnite (VPDB) Standard ($R_{standard}$).

To account for the effect of the atmospheric decline in the heavier isotope ^{13}C due to land–use changes and the effect of burning fossil fuel, which translates into the carbon isotope composition of wood rings, we calculated the carbon isotope discrimination ($\Delta^{13}C$) from the following equation (Farqhuar et al. 1989):

$$\Delta^{13}C\,(‰) = (\delta^{13}C_a - \delta^{13}C_r)/(1+\delta^{13}C_r) \quad (3)$$

where $\delta^{13}C_a$ and $\delta^{13}C_r$ are the carbon isotopic compositions of atmospheric CO_2 and of tree–ring, respectively. $\delta^{13}C_a$ was inferred by interpolating a range of data from Antarctic ice–core records, together with modern data from two Antarctic stations (Halley Bay and Palmer Station) of the CU–INSTAAR/NOAA–CMDL network for atmospheric CO_2 measurements, as first described in Ferrio et al. (2005). According to these records, the $\delta^{13}C_a$ value applied to tree–ring samples varied between −8.76‰ and −8.32‰.

To examine the extent by which high–frequency fluctuations of TRW could be explained by changes in $\Delta^{13}C$, we detrended the $\Delta^{13}C$ records using two alternative approaches: a) high–pass filtering using a cubic smoothing spline with a 50% frequency cut–off of 67 years followed by autocorrelation removal, and b) linear detrending followed by autocorrelation removal. The first approach was equivalent to the high–pass filtering used for TRW chronologies, whereas the second approach applied a less stringent filtering (i.e. greater stiffness) aimed at correcting essentially for the effect of the conspicuous warming trend occurring during the last 90 years on $\Delta^{13}C$ (Fig. 2). In both cases we obtained $\Delta^{13}C$ site chronologies consisting of stationary (mean = 1) dimensionless indices. The quality of the resulting site chronologies was evaluated by calculation of the same statistics used for TRW data (*Rbar*, *SNR*, *EPS*) from the 5 years for which the isotopes were measured on each tree separately. Finally, we combined site

$\Delta^{13}C$ records to produce a regional $\Delta^{13}C$ chronology as previously done for TRW records.

Using $\Delta^{13}C$ data, intrinsic water–use efficiency (WUEi) and intercellular CO_2 concentration (C_i) values were estimated according to:

$$WUE_i = (C_a \times (b - \Delta^{13}C)) / [1.6 \times (b - a)] \quad (4)$$

and

$$C_i = [(\Delta^{13}C - a) \times C_a] / (b - a) \quad (5)$$

where C_a represents the atmospheric CO_2 concentration, a is the fractioning during diffusion through stomata (~4.4‰) and b is the fractioning during carboxylation by Rubisco and PEP carboxylase (~27‰) (Farquhar et al. 1989). The factor 1.6 denotes the ratio of diffusivities of water vapour and CO_2 in the air. C_a values were taken from the National Oceanic and Atmospheric Administration (NOAA) Earth System Research Laboratory (http://www.esrl.noaa.gov/).

Theoretical WUEi values were calculated according to three scenarios as proposed by Saurer et al. (2004). Those scenarios describe how the C_i might follow the C_a increase over time: (a) either not at all, when C_i is maintained constant; (b) in a proportional way, when C_i/C_a is maintained constant; or (c) at the same rate, when $C_a - C_i$ is maintained constant (3). Initial C_i values were obtained for each site chronology by applying equation (5) to the average $\Delta^{13}C$ and C_a values of the first five years of the study period (1925–1929). We used these three scenarios to obtain theoretical WUEi values that were compared to WUEi records obtained from measured $\delta^{13}C$. To this end, the sum of squared differences between actual and predicted WUEi values (according to the different scenarios) was divided by the number of observations (years). The square root of this quantity is the root mean square predictive difference (RMS_{PD}), for which smaller values indicated more accurate theoretical predictions.

Total non–structural carbohydrate concentrations in sapwood

Wood cores from trees that were not examined for carbon isotopes were analysed for soluble sugars (SS) and starch concentrations. For this purpose the sapwood fraction of each core was separated, ground to fine powder and analysed twice. SS were extracted from 50 mg samples with 80% (v/v) ethanol. The extraction was done in a shaking water bath at 60 °C. After centrifugation, the concentration of SS was determined colourimetrically at 490 nm using the phenol–sulphuric method of Buysse and Merckx (1993). For starch concentration, the remaining sample in the undissolved pellet after ethanol extraction was digested with an enzyme mixture containing amyloglucosidase to reduce glucose as described in Palacio et al. (2007). Starch concentration was determined colourimetrically using the same method as for SS. Total non-structural carbohydrate concentrations (NSC, % dry matter) were calculated as the sum of SS and starch concentrations.

Meteorological data and climate analysis

Estimates of mean temperature, precipitation and the Standardized Precipitation Evapotranspiration drought index (SPEI; Vicente–Serrano et al. 2010) were obtained on a monthly basis from the high–resolution CRU TS3.22 dataset (Harris et al. 2014). The climate records, available on a 0.5º latitude/longitude grid basis for global land areas, covered the period 1925–2013. The monthly climate series averaged over the region 34º50'–35º00'N, 3°00'–3º50'E were used for further analyses.

The relationships between the regional TRW or $\Delta^{13}C$ chronologies and monthly climatic variables were assessed through bootstrapped correlations using the program

DendroClim2002 (Biondi and Waikul, 2004). These relationships were investigated from September of the previous year to October of the current year over the period of 1925–2013. Besides, this period was also split into two periods of approximate equal length (1925–1970 and 1971–2013) for which relationships between TRW or $\Delta^{13}C$ and monthly climatic variables were assessed separately. This strategy was adopted to investigate possible changes in trait–climate relationships in response to climate warming, a phenomenon that is especially noticeable from the 1970s onwards in the region (Fig. 2a).

Results

Regional climate, BAI and $\Delta^{13}C$ trends

The evolution of mean annual temperature indicated a consistent warming trend of 0.17°C per decade in the region during the period of 1925–2013 (Fig. 2a). Conversely, the precipitation pattern did not show a clear trend over the same period (Fig. 2b). However, a low–rainfall period coupled with high mean temperatures occurred at the turn of the 21st century, which translated into particularly low values for the SPEI drought index (Fig. 2c). Altogether, this pointed to increased intensity and duration of drought events in recent decades, although climate became comparatively more favourable during the last five years of the study period (Fig. 2c).

Long term radial–growth fluctuations at the site level are shown in Fig. 3 (left panels). For the common period with *EPS*> 0.85 across sites (1928–2013), the highest growth was observed in the Plateau site (mean BAI ± SE = 6.30 ± 0.27 cm^2 year^{-1}), followed by the South (5.74 ± 0.27 cm^2 year^{-1}) and North (3.99 ± 0.19 cm^2 year^{-1}) slopes. BAI significantly increased (P<0.05) across this period only in the North slope (regression slope = 0.038 cm^2 year^{-2}, R^2= 0.23). As a consequence, the differences in

BAI between sites decreased during the 21st century (period 2000–2013): 5.20 ± 0.33 cm^2 $year^{-1}$ (Plateau), 4.55 ± 0.35 cm^2 $year^{-1}$ (North slope), 5.41 ± 0.91 cm^2 $year^{-1}$ (South slope).

The evolution of site $\Delta^{13}C$ records is shown in Fig. 3 (right panels). The highest $\Delta^{13}C$ for the common period of 1925–2013 was observed in the North slope (mean $\Delta^{13}C$ ± SE = 16.14 ± 0.07 ‰), followed by the South slope and the Plateau sites (15.97 ± 0.08 ‰ and 15.50 ± 0.07 ‰, respectively). $\Delta^{13}C$ decreased significantly over time at each site, with slopes of the linear regression of $\Delta^{13}C$ on time ranging from –0.022 to –0.014 ‰ $year^{-1}$.

Tree–ring width and $\Delta^{13}C$ chronologies

The tree–ring width (TRW) chronologies showed good agreement regardless of differences in growing conditions among sites (e.g. slope aspect). In fact, the mean inter–series correlation of the regional chronology (*Rbar*= 0.46) was only slightly lower than that of each site chronology, which ranged from 0.47 to 0.68 (Table 1). Also, the signal–to–noise ratio (*SNR*) increased after combining all series into a regional master chronology (Table 1). By combining all available series, the length of the regional chronology having *EPS*> 0.85 was 169 years (period 1844–2013) (Table 1).

The $\Delta^{13}C$ records also showed good agreement among sites for the period of 1925–2013, as suggested by a high *Rbar* of the regional chronology (Table 1). At the site level, *Rbar* took similar or higher values than those found for TRW. There was also a higher temporal coherence in $\Delta^{13}C$ than in TRW records over the last 90 years for the region (i.e. higher *Rbar*) (Table 1). The regional $\Delta^{13}C$ chronology obtained using either a cubic smoothing spline or, alternatively, a linear detrending is shown in Fig. 4a.

The correlation between TRW and $\Delta^{13}C$ records after high–pass filtering (via cubic smoothing spline) was positive and significant (Fig. 4b). However, the relationship improved by using residuals from linearly detrended $\Delta^{13}C$ records (Fig. 4b), suggesting that the high–frequency information simultaneously retained in TRW and $\Delta^{13}C$ (i.e. inter–annual climate variability) was better retrieved by using different detrending strategies for each trait. Consequently, climate–$\Delta^{13}C$ relationships were examined using linearly detrended $\Delta^{13}C$ records.

Climate – growth relationships

The relationships between regional TRW and monthly climatic variables for the period of 1925–2013 are summarized in Fig. A3. TRW correlated negatively with previous autumn (September) and current spring-summer mean temperature (April, June to August). Besides, significant positive correlations were observed with winter-spring precipitation (January to May), and also with previous autumn (October) precipitation. The relationships involving SPEI drought index mirrored those of precipitation.

However, climate–growth relationships were not stable over time. For the period of 1925–1970, TRW correlated negatively with temperature in May, July and August (Fig. 5a) and positively with precipitation and SPEI only in late winter (February and March) and previous October (Fig. 5b,c). Conversely, the climatic influence on TRW was more important for the period of 1971–2013, especially for precipitation. TRW correlated negatively with temperature in summer (June and July) and also in the previous autumn (September) (Fig. 5a), and positively with precipitation and SPEI in September-October and from January to May (Fig. 5b,c).

$\Delta^{13}C$ – climate relationships

The relationships between regional $\Delta^{13}C$ and monthly climatic variables for the period of 1925–2013 are shown in Fig. A3. $\Delta^{13}C$ correlated negatively with late winter (February and March), summer (July and August) and October temperatures. Positive correlations were detected between $\Delta^{13}C$ and late winter to early spring precipitation (February to April) and between $\Delta^{13}C$ and previous October precipitation. The relationships involving SPEI resembled those of precipitation.

As for TRW, climate–$\Delta^{13}C$ relationships were not stable over time. $\Delta^{13}C$ correlated negatively with monthly temperatures only for the period of 1971–2013, particularly from previous November to current March (Fig. 5d). For the period of 1925–1970, $\Delta^{13}C$ correlated positively with precipitation and SPEI in late winter (February and March) and previous November (Fig. 5e,f). For the period of 1971–2013, $\Delta^{13}C$ was associated positively to March and April precipitation and SPEI (Fig. 5e,f).

Trends in WUEi

The mean WUEi across the period of 1925–2013 was significantly higher (P<0.05) at the Plateau site (106.2 μmol mol^{-1}) compared to the North and South sites (102.1 and 100.9 μmol mol^{-1} respectively). WUEi showed positive trends between 1925 and 2013 for all sites (Fig. 6). It increased by 29% (Plateau), 41% (North) and 46% (South) between the first (1925–1934) and the last decade (2005–2013) of the study period, with decadal increments of 4.2 μmol mol^{-1} (Plateau), 4.9 μmol mol^{-1} (North) and 5.0 μmol mol^{-1} (South). The comparison of time trends of $\Delta^{13}C$–based WUEi records against the three theoretical scenarios of WUEi change (C_i = ct, C_i/C_a = ct, $C_a - C_i$ = ct) indicated that the predictive power of the C_i/C_a = ct scenario was higher for the Plateau site (RMS_{PD}= 8 μmol mol^{-1}; Fig. 6a). Conversely, the North and South slope sites behaved closer to the C_i = ct scenario according to RMS_{PD} statistics (Fig. 6b,c). From the year

2000 onwards, however, there was an apparent change in WUEi trends, with trees showing no further stimulation to rising CO_2 (Fig. 6, left panels).

Changes in WUEi over time were related to BAI only in the North site, where a significant positive association (P<0.05) was detected between both parameters, although driven by some particular years of elevated WUEi and high BAI (2007, 2009 and 2010; Fig. 6e). Conversely, the relationship between WUEi and BAI was non–significant for the Plateau and South sites (Fig. 6d,f).

Carbon reserves in sapwood

Sapwood NSC was significantly higher (P<0.05) in the Plateau and South slope sites compared to the North slope stand (Fig. A4). This was due to higher concentrations in both SS and starch favouring especially the Plateau site. However, absolute differences in NSC among sites were small (less than 0.5%) with values ranging from 1.9 to 2.4% of sapwood dry matter.

Discussion

The Djelfa natural forests provide a unique ecological setting for anticipating the consequences of climate change on growth and functioning of Aleppo pine thriving in the southern Mediterranean Basin and, particularly, of the *ca*. 40–year old reforestations present in the Algerian Green Barrier. We found that the study Aleppo pine stands strongly enhanced their WUEi over the last 90 years. This finding is coherent with warmer conditions, intensified aridification and reduced pine performance (e.g. tighter stomatal control of water losses to prevent hydraulic failure), but the positive WUEi trends were largely uncoupled from changes in absolute growth, which remained essentially unaltered over time.

Contrasting BAI and $\Delta^{13}C$ trends over the last 90 years in the Saharan Atlas

The BAI patterns of natural Aleppo pine stands did not show a decreasing trend over the last century, indicating that warming-induced drought stress has not significantly affected secondary growth of pines in the area; instead, BAI trends were stable or even showed a significant increase in the case of the South slope site. The mean BAI values for the 21st century (4.5 – 5.2 cm^2 $year^{-1}$ across sites) are comparable to Aleppo pine individuals of similar characteristics as the trees we sampled for our study, growing under similar climatic conditions in the Mediterranean Basin e.g. 3.8 cm^2 $year^{-1}$ in the Ebro Valley, northeastern Spain (MAT= 14.8°C, MAP= 325 mm., Sangüesa–Barreda et al. (2015)) or 4.8 cm^2 $year^{-1}$ in Yatir forest, Israel (MAT= 18.0°C, MAP= 285 mm, Klein et al. (2014)). These Aleppo pines from Spain and Israel also did not show a decreasing BAI trend over the last 40 years, except for severely drought–stressed trees in Yatir. In contrast, individual BAI values were substantially lower than the mean BAI (>10 cm^2 $year^{-1}$) of Aleppo pine natural stands growing at similar altitude but under colder and more mesic conditions in eastern Spain (MAT= 10.5°C, MAP~ 460 mm; Camarero et al. 2015).

Unlike BAI, $\Delta^{13}C$ values showed a pronounced decreasing trend (mean slope across sites= –0.019 ‰ $year^{-1}$), indicating enhanced WUEi over the period of 1925–2013. As any increase in WUEi resulting from an increase in C_a (i.e. CO_2 fertilization) is limited to maintain a constant C_i/C_a ratio (i.e. a constant $\Delta^{13}C$ over time; see eq. [5]) (McCarroll et al. 2009), our results suggest that pines from the Saharan Atlas are not only responding to rising CO_2 concentrations, but also to warming-induced drought stress limiting stomatal conductance and, hence, decreasing carbon uptake. In fact, the

observed negative $\Delta^{13}C$ trend concurs with the steady increase in MAT observed during the last 90 years. Such warming trend and associated drought is likely to increasingly impact tree ecophysiology by decreasing water losses through a progressively tighter stomatal regulation. For the sake of comparison, the Djelfa $\Delta^{13}C$ chronology is drawn together with two Aleppo pine $\Delta^{13}C$ chronologies from the western Mediterranean Basin having similar bioclimatic conditions (Fig. A5). Contrasting with Djelfa, these time series exhibit a flat $\Delta^{13}C$ response over the last 60 years. A few studies in conifers have also shown significant decreasing $\Delta^{13}C$ trends over the 20th century, although lower than that reported here, e.g -0.008 ‰ year^{-1} (*Pinus sylvestris* from northwestern Spain; Andreu–Hayles et al. 2011) or -0.003‰ year^{-1} (*Fitzroya cupressoides* from southern Chile; Urrutia–Jalabert et al. 2015). An exception is the case of *Abies alba* forests from the Spanish Pyrenees showing drought–induced dieback (-0.021‰ year^{-1}; Linares and Camarero, 2012). In all these cases, trees exhibited a significant decrease in radial growth over the 20th century that is not observed in our study. Indeed, the long–term uncoupling between ecophysiological performance and secondary growth of Aleppo pine suggests a high resilience to warming-induced drought stress for this Mediterranean conifer.

Changing climate – growth associations do not influence absolute growth of Pinus halepensis

Overall, Aleppo pine TRW was constrained by warm conditions during the previous autumn, and also during current spring and summer. The negative relationships of growth with warm temperatures during most of the growing season (April, June to August) exemplify the impact of drought stress for a highly plastic species such as Aleppo pine (De Luis et al. 2013), which behaves opportunistically when conditions

become favourable for growth (e.g. under low vapour pressure deficit) (Ferrio et al. 2003). A negative influence of warm autumn (September) temperatures is often interpreted as an indication of carbon reserves depletion that are otherwise used for the formation of a new ring, resulting in low secondary growth (Kagawa et al. 2006). The positive correlation of TRW with previous October precipitation has been attributed to polycyclism, the ability of Aleppo pine to produce several flushes in the same growing season (Touchan et al. 2016). A rainy winter–spring period (January to May) was also positively associated with TRW. Most rainfall is concentrated in winter and spring in the Saharan Atlas, with long dry periods during the summer whose scarce precipitation appears as irrelevant for tree growth, suggesting cambial quiescence during the dry summer (Camarero et al. 2010; Touchan et al. 2012). Trees responded in a similar way to fluctuations in the SPEI drought index, indicating that monthly SPEI is mainly driven by rainfall variation under severe drought conditions. However, the warming trend occurring over the last 90 years changed the dependence of tree growth on climate factors in the Saharan Atlas, suggesting a rising influence of drought stress through increased evapotranspiration. In particular, the previous TRW dependence on late winter precipitation expanded to early winter (January) and spring, whose precipitation is nowadays critical to sustain Aleppo pine growth. This outcome indicates an intensifying influence of increasing growing season aridity on pine performance.

Notably, these recent changes in climate responses linked to increased aridity have not caused the decline of Aleppo pine growth, as suggested by BAI trends. Similarly, bark beetle infested Aleppo pine individuals were able to sustain their growth compared to healthy trees (Sangüesa–Barreda et al. 2015), and only severely drought–stressed individuals presented a substantial BAI decrease in the last decades (Klein et al. 2014). These results are intriguing and do not concur with previous findings on the

Mediterranean Basin, where negative growth trends are usually reported for forest trees since the 1970s (Galván et al. 2014; Shestakova et al. 2016). In fact, sapwood NSC (~2%) suggests lack of source limitation in the studied stands, as these were comparable with those obtained in other studies performed under optimal (~1.5% in *Pinus sylvestris*; Hoch et al. 2003) and sub–optimal water conditions (~3.3% in *Pinus halepensis*; unpublished).

The uncoupling between physiological sensitivity to climate change and growth stability might be partly explained by a change in phenology triggered by increasingly warm and dry conditions. For an extremely plastic conifer such as Aleppo pine, the actual growing season may be shifting towards earlier months in winter– early spring without reducing tree growth (Bigelow et al. 2014). This species shows two periods with reduced cambial activity associated with summer drought (Camarero et al. 2010) and low winter temperatures (Liphschitz and Lev–Yadun, 1986). The recent TRW dependence on January precipitation supports this hypothesis, which would make growth more reliant on water availability at the very early growing season, a period progressively more suitable for tree performance as climate becomes warmer and drier.

Changing climate –$\Delta^{13}C$ associations concur with the decreasing $\Delta^{13}C$ trend

$\Delta^{13}C$ showed a good agreement among series which translated into a stronger regional signal (*Rbar*) than for TRW. This result suggests that, despite micro–environmental influences, carbon isotopes (as surrogates of the tree's carbon and water balance) are better tracers of regional climate signals than radial growth (McCarroll and Loader, 2004; Andreu et al. 2008). However, both proxies can be regarded as complementary as they often contain different or partially overlapping climatic information, as shown for Spanish pinewoods (Ferrio et al. 2003; Andreu et al. 2008). This is actually the case in

our study (*cf*. Fig. 4), in which the climate analysis revealed delayed TRW responses to climate factors (especially temperature) as compared to $\Delta^{13}C$ (Fig. A3).

As for TRW, the warming trend also coincided with a change in the dependence of $\Delta^{13}C$ on climate. On one hand, the negative $\Delta^{13}C$ sensitivity to warm winter temperatures observed at the turn of this century indicates increasing climate dependence of gas exchange processes during the early growing season, hence suggesting increased winter carbon uptake and, perhaps, an advanced cambial onset (Bigelow et al. 2014). On the other hand, the delayed precipitation signal (April) in the last decades compared to the mid twentieth century may suggest increased sensitivity to drier springs, a period of high precipitation and favourable temperatures for growth in the region. The amplified sensitivity to climate in the peak of the growing season (spring) is also suggested by the steady decrease in $\Delta^{13}C$ over the last 90 years, which indicates increasingly harsher conditions for tree performance, as already reported across water availability gradients for Aleppo pine (Del Castillo et al. 2015). These ideas could be confirmed through a detailed analysis of the onset, ending and duration of xylogenesis. In this regard, the presumed shift in phenology towards earlier months, triggered by climate change, did not suffice to counterbalance the worsening in spring–summer growing conditions as reflected in progressively lower $\Delta^{13}C$ records, forcing a strong physiological reaction in terms of enhanced WUEi.

A strong physiological response to warming in Aleppo pine

WUEi increased by *ca*. 39% across sites between 1925 and 2013 (88 years). This substantial increment cannot be exclusively attributed to a rise of atmospheric CO_2, but also to an active reaction of trees to increasing temperatures and drought stress boosting WUEi (e.g. McCarroll et al. 2009; Frank et al. 2015). In a widespread survey of WUEi

trends in European forests over the 20th century, Saurer et al. (2014) reported equivalent increments to those of our study (i.e. ≥44% in 100 years) in only two out of 35 study sites, which corresponded to *Abies alba* (south Germany) and *Quercus robur* (south Finland) stands. This huge reaction to the combined effects of CO_2 fertilization and climate warming is indicated by the dominance of Aleppo pine responses consistent with a low sensitivity of C_i to C_a (i.e. C_i= ct scenario), which are barely reported in the literature (e.g. Hereş et al. (2014) in *Pinus sylvestris*; Linares and Camarero (2012) in *Abies alba*) compared to less drastic physiological adjustments to CO_2 increases. Overall, our results indicate that drought–induced stomatal closure has reduced transpiration and, hence, augmented WUEi in Aleppo pine from the Saharan Atlas, but not at the cost of reduced radial growth (*cf*. Fig. 6).

However, the observed stimulation in WUEi seems to have slowed down or even ceased from the year 2000 onwards (*cf*. Fig. 6, left panels). This effect has been reported elsewhere (e.g. Peñuelas et al. (2008); Linares and Camarero (2012)) and can be interpreted as the result of trees getting to a physiological threshold in its ability to increase WUEi as CO_2 rises due to drought–induced stomatal closure. Most worrying is the fact that, often, conifers in deteriorating health show such limited responsiveness to increasing CO_2 as compared with their non–declining counterparts (e.g. Hereş et al. (2014); Linares and Camarero (2012)). Hence, such recent turnaround in Aleppo pine might anticipate die–back episodes in the following years.

Implications for future performance and management of Aleppo pine plantations in the Algerian Green Barrier

The Algerian Green Barrier consists basically of Aleppo pine reforestations planted at a very high density (2,000 trees ha^{-1}). The high competition for water, together with the use of non–autochthonous seed sources originating from the Algerian coast (Bensaïd, 1995), may explain the harmful incidence of the pine processionary moth (*Thaumetopoea pityocampa*), which is severely defoliating most plantations from the Djelfa region (notably, the natural stands remain mainly pest–free). It is therefore likely that drought stress acts as inciting factors (*sensu* Manion, 1991) by weakening host pines and exacerbating damage due to the presence of the moth. The current ecophysiological performance of the natural Aleppo pine stands in the region, as characterized in this study, asks for urgent management practices to ameliorate the water status of such over dense plantations. Among those, thinning increases the availability of water, light and nutrients. Recent studies in conifers, including Aleppo pine, indicate long–term growth enhancements due to increases in stomatal conductance and associated enhanced water availability (i.e. less negative stem water potentials) after thinning (Moreno–Gutiérrez et al. 2011; Caley et al. 2016; Giuggiola et al. 2016). Thus, high-intensity thinning (≥50% BA removal; Caley et al. 2016) may be the most imperative measure towards mitigating the effects of further aridification in the region's forests, although WUEi may be unaffected because is mainly driven by CO_2 and climate rather than by competition (Fernández de Uña et al. 2016).

In conclusion, our study highlights the substantial plasticity of Aleppo pine to warming-induced drought stress. This is indicated by the lack of reduction in radial growth over the period of 1925-2013, while $\Delta^{13}C$ records decreased by *ca*. 2‰, pointing to huge increases in WUEi (~39%). The extent of such plastic responses for Aleppo

pines growing at the southernmost limit of the species distribution area is, from a physiological point of view, remarkable. As previously mentioned, it is however unlikely to expect a similar pace in the degree of physiological adjustments of Aleppo pine for the near future. Wood $\Delta^{13}C$ values below 15‰ are hardly documented for Aleppo pine (Del Castillo et al. 2015), which suggests that regional forests may be reaching a physiological threshold (i.e. WUEi asymptote), hence compromising the future of such fragile ecosystems. The prediction of these critical thresholds becomes an urgent research priority for Mediterranean forestry.

References

Andreu L, Planells O, Gutiérrez E, Helle G, Schleser G H (2008) Climatic significance of tree–ring width and $\delta^{13}C$ in a Spanish pine forest network. Tellus B 60: 771–781.

Andreu–Hayles L, Planells O, Gutiérrez E, Muntan E, Helle G, Anchukaitis KJ, Schleser GH (2011) Long tree–ring chronologies reveal 20th century increases in water–use efficiency but no enhancement of tree growth at five Iberian pine forests. Glob Change Biol 17: 2095–2112.

Barbéro M, Loisel R, Quézel P, Richardson DM, Romane F (1998) Pines of the Mediterranean Basin. In: Ecology and Biogeography of *Pinus*, Richardson DM (ed). Cambridge University Press: Cambridge, pp 153–170.

Benalia S (2009) The Green Barrier in Algeria: Actual Situation and Development Prospect. In: "Technology and management to ensure sustainable agriculture, agro–systems, forestry and safety", XXXIII CIOSTA – CIGR V Conference 2009, Reggio Calabria (Italy) and IUFRO (Unit 3.06.00) Workshop, pp. 2163–2166.

Bensaïd S (1995) Bilan critique du barrage vert en Algérie. Science et Changements Planétaires/Sécheresse 6 : 247–255.

Berger A, Guiot J, Mathieu L, Munaut A (1979) Cedar tree–rings and climate in Morocco. Tree– Ring Bull 39: 61–75.

Bigelow SW, Papaik MJ, Caum C, North MP (2014) Faster growth in warmer winters for large trees in a Mediterranean–climate ecosystem. Clim Change 123: 215–224.

Biondi F, Waikul K (2004) DENDROCLIM 2002: a C++ program for statistical calibration of climate signals in tree–ring chronologies. Computers & Geosciences 30: 303–311.

Buysse J, Merckx R (1993) An improved colorimetric method to quantify sugar content of plant tissue. J Exp Bot. 44: 1627–1629.

Caley A, Zoref C, Tzukerman M, Moshe Y, Zangy E, Osem Y (2016) High-intensity thinning treatments in mature *Pinus halepensis* plantations experiencing prolonged drought. Eur J Forest Res. doi 10.1007/s10342-016-0954-y.

Camarero JJ, Olano JM, Parras A (2010) Plastic bimodal xylogenesis in conifers from continental Mediterranean climates. New Phytol 185: 471–480.

Camarero JJ, Gazol A, Sangüesa–Barreda G, Oliva J, Vicente–Serrano SM (2015) To die or not to die: early warnings of tree dieback in response to a severe drought. J Ecol 103: 44–57.

Cherubini P, Gartner BL, Tognetti R, Braüker OU, Schoch W, Innes JL (2003) Identification, measurement and interpretation of tree rings in woody species from Mediterranean climates. Biol Rev 78: 119–148.

Chbouki N, Stockton CW, Myers DE (1995) Spatiotemporal patterns of drought in Morocco. Int J Climatol 15:187–205.

Cook ER, Peters K (1981) The smoothing spline: a new approach to standardize forest interior tree–ring width series for dendroclimatic studies. Tree–Ring Bull 41: 45–53.

Cook ER, Krusic PJ (2005) Program ARSTAN: A tree–ring standardization program based on detrending and autoregressive time series modeling, with interactive graphics. Columbia University, Palisades, New York.

Cook BI, Anchukaitis KJ, Touchan R, Meko DM, Cook ER (2016) Spatiotemporal drought variability in the Mediterranean over the last 900 years. J Geophys Res Atmos 121: 2060–2074.

De Luis, M., Novak, K., Raventós, J., Gricar, J., Prislan, P., Cufar, K., 2011. Climate factors promoting intra–annual density fluctuations in Aleppo pine (*Pinus halepensis*) from semiarid sites. Dendrochronologia, 29, 163–169.

De Luis M, Čufar K, Di Filippo A, Novak K, Papadopoulos A, Piovesan G, Rathgeber

CBK, Raventós J, Saz MA, Smith KT (2013) Plasticity in dendroclimatic response across the distribution range of Aleppo pine (*Pinus halepensis*). PLoS One 8, e83550.

Del Castillo J, Voltas J, Ferrio JP (2015) Carbon isotope discrimination, radial growth, and NDVI share spatiotemporal responses to precipitation in Aleppo pine. Trees–Struct Funct 29: 223–233.

EFI (European Forest Institute), Palahí M, Birot Y, Bravo F, Gorriz E (2009) Modelling, valuing and managing Mediterranean forest ecosystem for non–timber goods and service. Proceedings No.57, Joensuu, Finland.

Esper J, Frank D, Buntgen U, Verstege A, Luterbacher J, Xoplaki E (2007) Long–term drought severity variations in Morocco. Geophys Res Lett 34, L17702.

Farquhar GD, Ehleringer J, Hubick K (1989) Carbon isotope discrimination and photosynthesis. Annu Rev Plant Phys 40: 503–537.

Fernández de Uña L, McDowell NG, Cañellas I, Gea-Izquierdo G (2016) Disentangling the effect of competition, CO_2 and climate on intrinsic water-use efficiency and tree growth. J Ecol 104: 678-690.

Ferrio JP, Florit A, Vega A, Serrano L, Voltas J (2003). $\Delta^{13}C$ and tree–ring width reflect different drought responses in *Quercus ilex* and *Pinus halepensis*. Oecologia 137: 512–518.

Ferrio JP, Araus JL, Buxó R, Voltas J, Bort J (2005) Water management practices and climate in ancient agriculture: inferences from the stable isotope composition of archaeobotanical remains. Veg Hist Archaeobot 14: 510–517.

Ferrio JP, Voltas J (2005) Carbon and oxygen isotope ratios in wood constituents of *Pinus halepensis* as indicators of precipitation, temperature and vapour pressure deficit. Tellus B 57: 164-173.

Frank DC, Poulter B, Saurer M, et al. (2015) Water–use efficiency and transpiration across European forests during the Anthropocene. Nat Clim Change 5: 579–584.

Galván JD, Camarero JJ, Ginzler C, Büntgen U (2014) Spatial diversity of recent trends in Mediterranean tree growth. Environ Res Lett 9(8), 084001.

Galván JD, Büntgen U, Ginzler C, Grudd H, Gutiérrez E, Labuhn I, Camarero JJ (2015) Drought–induced weakening of growth–temperature associations in high–elevation Iberian pines. Global Planet. Change 124, 95–106.

Gessler A, Ferrio JP, Hommel R, Treydte K, Werner RA, Monson RK (2014) Stable isotopes in tree rings: towards a mechanistic understanding of isotope fractionation and mixing processes from the leaves to the wood. Tree Physiol 34: 796–818.

Giorgi F, Lionello P (2008) Climate change projections for the Mediterranean region. Global Planet Change 63: 90–104.

Giuggiola A, Ogée J, Rigling A, Gessler A, Bugmann H, Treydte K (2016) Improvement of water and light availability after thinning at a xeric site: which matters more? A dual isotope approach. New Phytol 210: 108–121.

Harris I, Jones PD, Osborn TJ, Lister DH (2014) Updated high–resolution grids of monthly climatic observations – the CRU TS3.10 Dataset. Int J Climatol 34: 623–642.

Hereş AM, Voltas J, Claramunt–López B, Martínez–Vilalta J (2014) Drought–induced mortality selectively affects Scots pine trees that show limited intrinsic water–use efficiency responsiveness to raising atmospheric CO_2. Funct Plant Biol 41: 244–256.

Hoch G, Richter A, Körner C (2003) Non–structural carbon compounds in temperate forest trees. Plant Cell Environ 26: 1067–1081.

Hoerling M, Eischeid J, Perlwitz J, Quan X, Zhang T, Pegion P (2012) On the increased frequency of Mediterranean drought. J Clim 25: 2146–2161.

Holmes RL (1983) Computer–assisted quality control in tree–ring dating and measurement.Tree–Ring Bull 43: 69–78.

Kagawa A, Sugimoto A, Maximov TC (2006) $^{13}CO_2$ pulse–labelling of photo assimilates reveals carbon allocation within and between tree rings. Plant Cell Environ 29: 1571–1584.

Klein T, Hoch G, Yakir D, Korner C (2014) Drought stress, growth and nonstructural carbohydrate dynamics of pine trees in a semi–arid forest. Tree Physiol 34: 981–992.

Leavitt SW (2008) Tree–ring isotopic pooling without regard to mass: No difference from averaging $\delta^{13}C$ values of each tree. Chem Geol 252: 52–55.

Linares JC, Camarero JJ (2012) From pattern to process: linking intrinsic water–use efficiency to drought–induced forest decline. Glob Change Biol 18: 1000–1015.

Liphschitz N, Lev–Yadun S (1986) Cambial activity of evergreen and seasonal dimorphics around the Mediterranean. IAWA Bull 7: 145–153.

Manion PD (1991) Tree Disease Concepts. New York.

McCarroll D, Loader NJ (2004) Stable isotopes in tree rings. Quaternary Sci Rev 23: 771–801.

McCarroll D, Gagen MH, Loader NJ, Robertson I, Anchukaitis, KJ, Los S, Young GHF, Jalkanen R, Kirchhefer A, Waterhouse JS (2009) Correction of tree ring stable carbon isotope chronologies for changes in the carbon dioxide content of the atmosphere. Geochim Cosmochim Ac 73: 1539–1547.

McDowell N, Pockman WT, Allen CD, Breshears DD, Cobb N, Kolb T, Plaut J, Sperry J, West A, Williams DG, Yepez EA (2008) Mechanisms of plant survival and mortality during drought: why do some plants survive while others succumb to drought? New Phytol 178: 719–739.

Mitrakos K (1980) A theory for Mediterranean plant–life. Oekol Plant 15: 245–252.

Moreno–Gutiérrez C, Barbera GG, Nicolás E, De Luis M, Castillo VM, Martínez–Fernandez F, Querejeta JI (2011) Leaf $\delta^{18}O$ of remaining trees is affected by thinning intensity in a semiarid pine forest. Plant Cell Environ 34: 1009–1019.

Munaut AV (1978) Dendroclimatological studies on cedars in Morocco. In: Evolution of Planetary Atmospheres and Climatology of the Earth, Paris, France, 373–379.

Novak K, de Luis M, Saz MA, Longares LA, Serrano-Notivoli R, Raventós J, Cûfar K, Gričar J, Di Filippo A, Piovesan G, Rathgeber CBK, Papadopoulos A, Smith KT (2016) Missing rings in *Pinus halepensis* – The missing link to relate the tree-ring record to extreme climatic events. Front Plant Sci 7, art. 727.

Pacheco A, Camarero JJ, Carrer M (2016) Linking wood anatomy and xylogenesis allows pinpointing of climate and drought influences on growth of coexisting conifers in continental Mediterranean climate. Tree Physiol. 10.1093/treephys/tpv125.

Palacio S, Maestro M, Montserrat–Martí G (2007) Seasonal dynamics of non–structural carbohydrates in two species of Mediterranean sub–shrubs with different leaf phenology. Environ Exp Bot 59: 34–42.

Peñuelas J, Hunt JM, Ogaya R, Jump AS (2008) Twentieth century changes of tree–ring$\delta^{13}C$ at the southern range–edge of *Fagus sylvatica*: increasing water–use efficiency does not avoid the growth decline induced by warming at low altitudes. Glob Change Biol 14: 1–13.

Sangüesa–Barreda G, Camarero JJ, Oliva J, Montes F, Gazol A (2015) Past logging, drought and pathogens interact and contribute toforest dieback. Agric For Meteorol 208: 85–94.

Santos–del–Blanco L, Bonser SP, Valladares F, Chambel MR, Climent J (2013) Plasticity in reproduction and growth among 52 range–wide populations of a

Mediterranean conifer: Adaptive responses to environmental stress. J Evolution Biol 26: 1912–1924.

Saurer M, Siegwolf R, Schweingruber F (2004) Carbon isotope discrimination indicates improving water–use efficiency of trees in northern Eurasia over the last 100 years. Glob Change Biol 10: 2109–2120.

Saurer M, Spahni R, Frank DC, et al. (2014) Spatial variability and temporal trends in water–use efficiency of European forests. Glob Change Biol 20: 3700–3712.

Schiller G (2000) Ecophysiology of *Pinushalepensis* Mill.and*P. brutia* Ten. In: Ne'eman G, Trabaud L, eds. Ecology, biogeography and management of *Pinus halepensis* and *P. brutia* forest ecosystems in the Mediterranean basin. Leiden, the Netherlands: Backhuys Publishers pp. 51–65.

Shestakova TA, Aguilera M, Ferrio JP, Gutiérrez E, Voltas J (2014) Unravelling spatiotemporal tree–ring signals in Mediterranean oaks: a variance–covariance modelling approach of carbon and oxygen isotope ratios. Tree Physiol 34: 819–838.

Shestakova TA, Gutiérrez E, Kirdyanov AV, Camarero JJ, Génova M, Knorre AA, Linares JC, Resco de Dios V, Sánchez–Salguero R, Voltas J (2016) Forests synchronize their growth in contrasting Eurasian regions in response to climate warming. P Natl Acad Sci USA 113: 662–667.

Thuiller W, Lavorel S, Araujo MB, Sykes MT, Prentice IC (2005) Climate change threats to plant diversity in Europe. P Natl Acad Sci USA 102: 8245–8250.

Till C, Guiot J (1990) Reconstruction of precipitation in Morocco since 1100 A.D. based on *Cedrus atlantica* tree–ring widths. Quaternary Res 33: 337–351.

Touchan R, Meko DM, Aloui A (2008) Precipitation reconstruction for Northwestern Tunisia from tree rings. J Arid Environ 72: 1887–1896.

Touchan R, Anchukaitis KJ, Meko DM, Sabir M, Attalah S, Aloui A (2011)

Spatiotemporal drought variability in northwestern Africa over the last nine centuries. Clim Dynam 37: 237–252.

Touchan R, Shishov VV, Meko DM, Nouiri I, Grachev A (2012). Process based model sheds light on climate sensitivity of Mediterranean tree–ring width. Biogeosciences 9: 965–972.

Touchan R, Kherchouche D, Oudjehih B, Touchan H, Slimani S, Meko DM (2016) Dendroclimatology and wheat production in Algeria. J Arid Environ 124: 102-110.

Urrutia–Jalabert R, Malhi Y, Barichivich J, Lara A, Delgado–Huertas A, Rodríguez CG, Cuq E (2015) Increased water use efficiency but contrasting tree growth patterns in *Fitzroya cupressoides* forests of southern Chile during recent decades. J Geophys Res Biogeosci 120: 2505–2524,

Vicente–Serrano SM, Beguería S, López–Moreno JI (2010) A multi–scalar drought index sensitive to global warming: The Standardized Precipitation Evapotranspiration Index – SPEI. J Clim 23: 1696–1718.

Voltas J, Lucabaugh D, Chambel MR, Ferrio JP (2015) Intraspecific variation in the use of water sources by the circum–Mediterranean conifer *Pinus halepensis*. New Phytol 208: 1031–1041.

Wigley TML, Briffa KR, Jones PD (1984) On the average value of correlated time series, with applications in dendroclimatology and hydrometeorology. J Appl Meteor Climatol 23: 201–213.

FIGURE CAPTIONS

Fig. 1 Distribution area of *Pinus halepensis* in the western Mediterranean basin showing the location of the three sampling sites in the Saharan Atlas region of Algeria and climate diagram obtained from the high–resolution CRU TS3.22 dataset, where the data were averaged over the region 34º50'–35º00' N, 3°00'–3º50' E (1925–2013 period).

Fig. 2 Temporal evolution of main climate factors for the period of 1901–2013: a) mean annual temperature (MAT), b) mean annual precipitation (MAP) and c) Standardised Precipitation–Evapotranspiration Index (SPEI). The linear trend for temperature is significant at $P<0.05$. The horizontal line for precipitation indicates the average value of the historical series.

Fig. 3 Left panels: Evolution of basal area increments (BAI, means ± standard error) at the site level. The dotted vertical lines show the year in which the Expressed Population Signal (*EPS*) was above the 0.85 threshold. Right panels: Carbon isotope discrimination ($\Delta^{13}C$) time series of the study sites for the common 1925–2013 period. Sites: a, d) Plateau; b, e) North slope; c, f) South slope

Fig. 4 a) Regional chronologies for tree–ring width (TRW; black line) and carbon isotope discrimination ($\Delta^{13}C$) indices. $\Delta^{13}C$ records were subjected to high–pass filtering (cubic smoothing spline with a 50% frequency cut–off of 67 years, red line) and linear detrending (blue line). b) Relationships between standardized TRW and $\Delta^{13}C$ records (red dots, high–pass filtering; blue dots, linear detrending) (***: $P<0.001$).

Fig. 5 Tree–ring width (left panels) and carbon isotope discrimination ($\Delta^{13}C$) (right panels) responses to climate. Relationships with climate are based on bootstrapped correlations between tree–ring indices (obtained by cubic smoothing spline with a 50% frequency cut–off of 67 years for ring–width and by linear detrending for $\Delta^{13}C$) and monthly mean temperature, precipitation and Standardized Precipitation Evapotranspiration Index (SPEI) at the 1–month scale for the periods of 1925–1970 (red bars) and 1970–2013 (blue bars). Monthly mean temperatures were linearly detrended to eliminate the effect of the warming trend from the temporal series; therefore, correlations with tree–ring indices were performed using residuals of linear trends. Significant correlation coefficients (P<0.05) are indicated by filled bars. Lowercase and uppercase letters on the *x*–axes correspond to the months before and during tree–ring formation, respectively.

Fig. 6 Left panels: Temporal trends in intrinsic water–use efficiency (WUEi) as related to three conceptual models assuming a constant intercellular CO_2 concentration (C_i=ct scenario), a constant ratio between intercellular and atmospheric CO_2 concentrations (C_i/C_a= ctn scenario), and a constant difference between atmospheric and intercellular CO_2 concentrations ($C_a–C_i$= ctn scenario). The root mean square of the predicted difference (actual minus predicted values; RMS_{PD}) is shown for each model. The grey areas highlight the period of 2000–2013 when WUEi shows no increasing trend over time. Right panels: Relationships between WUEi and basal area increment (BAI). A linear trend denotes a significant association (**: P<0.01). a, d) Plateau; b, e) North slope; c, f) South slope.

Table 1. Sampling sites features and descriptive statistics of chronologies for tree–ring width (TRW) and carbon isotope discrimination ($\Delta^{13}C$) indices of *Pinus halepensis*at the natural forest area of Sénalba Chergui, Djelfa province (Saharan Atlas, Algeria). Descriptive statistics are calculated for TRW and $\Delta^{13}C$indices using a cubic smoothing spline with a 50% frequency cut–off of 67 years. Results for the combined (regional) master chronology are also included. The variability of mean values is expressed as standard deviation (± SD). Abbreviations: DBH, diameter at breast height; *Rbar*, mean inter–series correlation; *SNR*, signal to noise ratio; *EPS*, expressed population signal.

								TRW				$\Delta^{13}C$ (1925–2013)			
Site id. (slope aspect)	**Site name**	**Lat. (N)**	**Long. (E)**	**Altitude (m)**	**DBH (cm)**	**Height (m)**	**Time span**	**No. trees**	***EPS* > 0.85 since**	***Rbar***	***SNR***	**No. trees**	***EPS***	***Rbar***	***SNR***
Plateau	Toughersan	34°32'	3°02'	1400	24.5±4.0	14.7±2.4	1868–2013	11	1928	0.47	4.55	5	0.83	0.49	4.82
North	Theniat Enser	34°37'	3°06'	1365	21.7±1.9	18.1±1.8	1847–2013	12	1883	0.63	34.03	5	0.98	0.90	45.01
South	Theniat Enser	34°36'	3°05'	1360	22.6±3.7	17.9±2.3	1830–2013	47	1844	0.68	41.80	5	0.87	0.57	6.64
Combined							1830–2013	70	1844	0.46	70.71	15	0.89	0.72	51.02

Figure 1

Click here to download Figure Fig. 1.tif

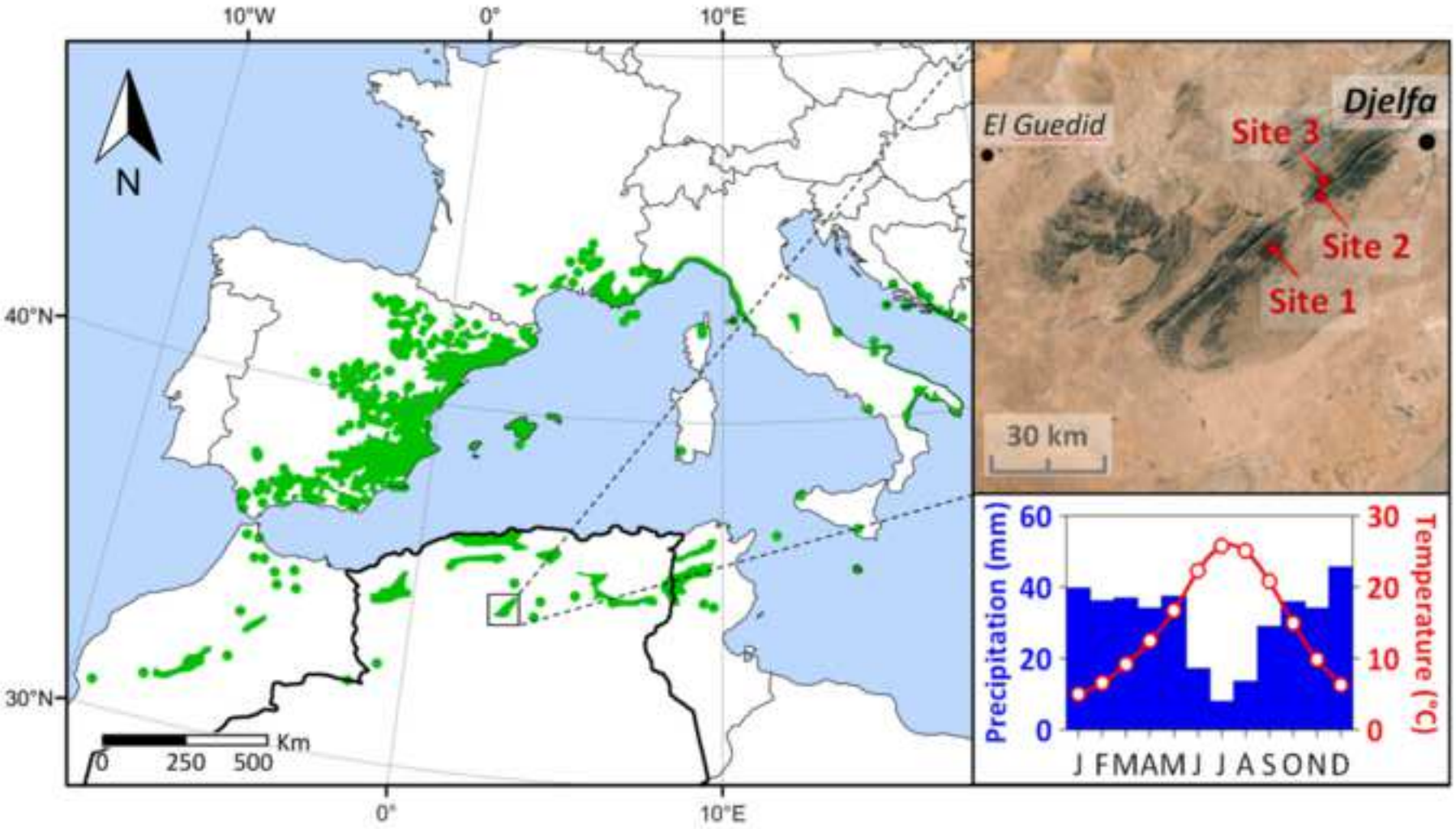

Figure 2

Click here to download Figure Fig2.TIF

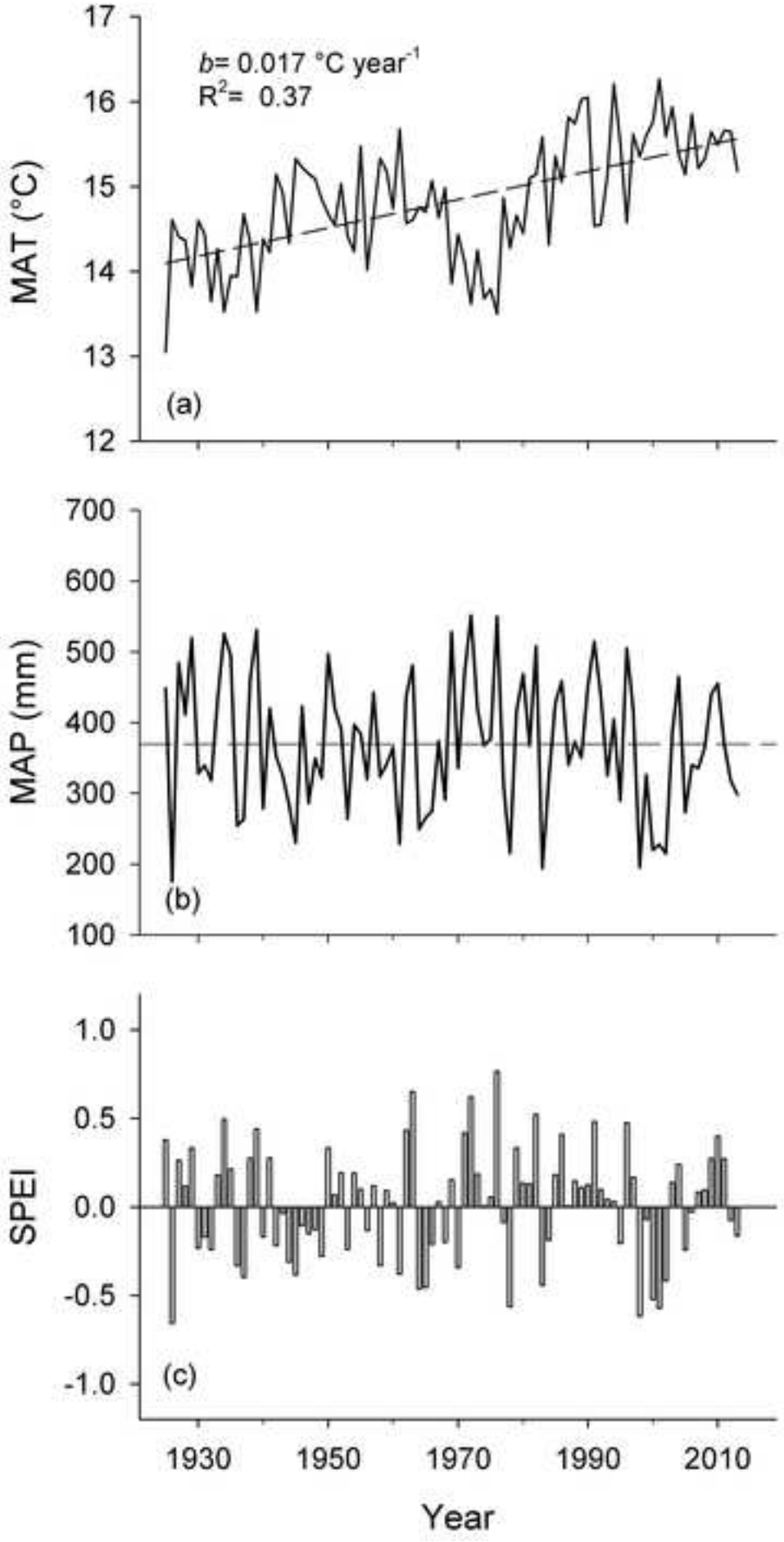

Figure 3

Click here to download Figure Fig3.TIF

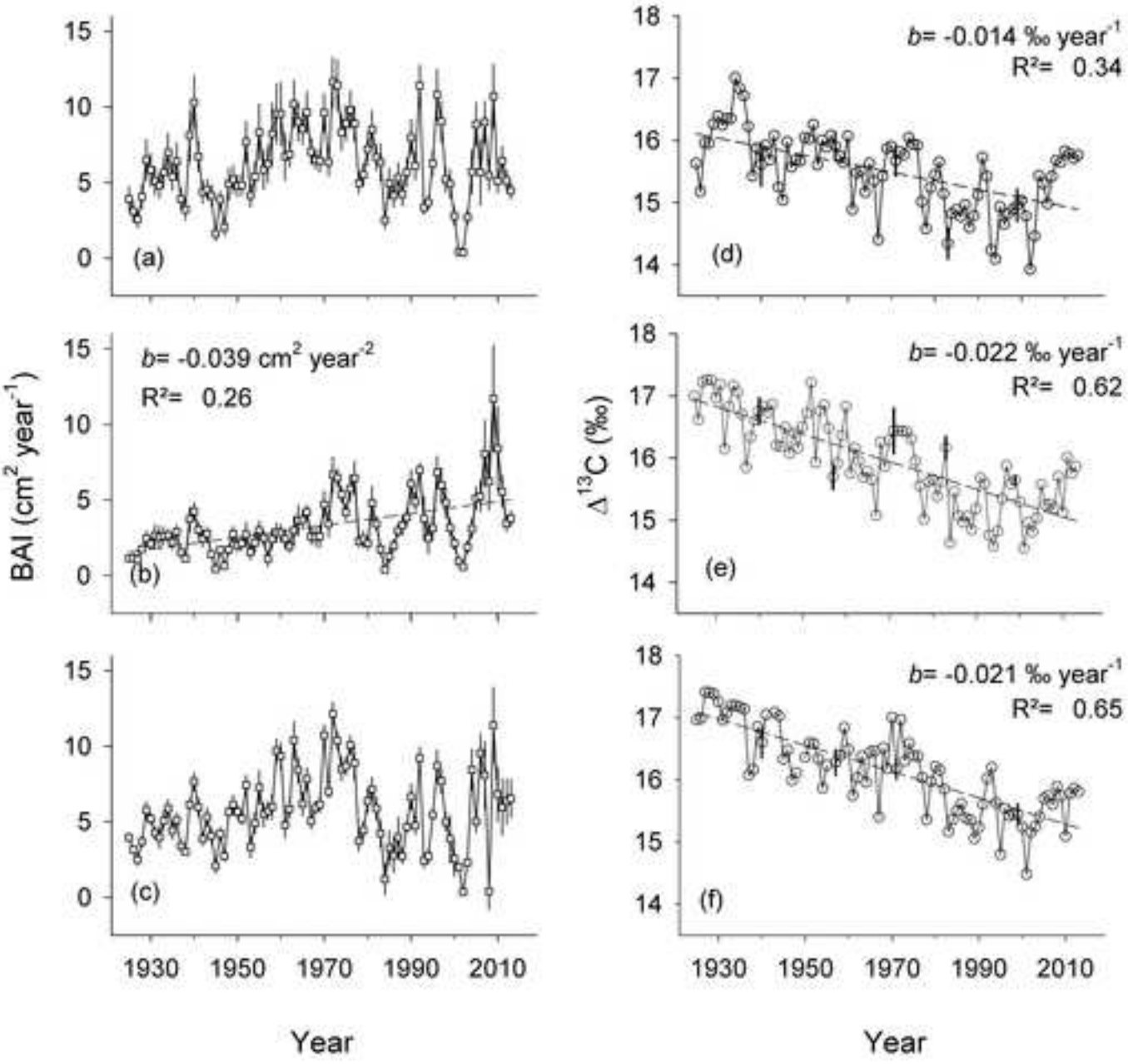

Figure 4

Click here to download Figure Fig4.TIF

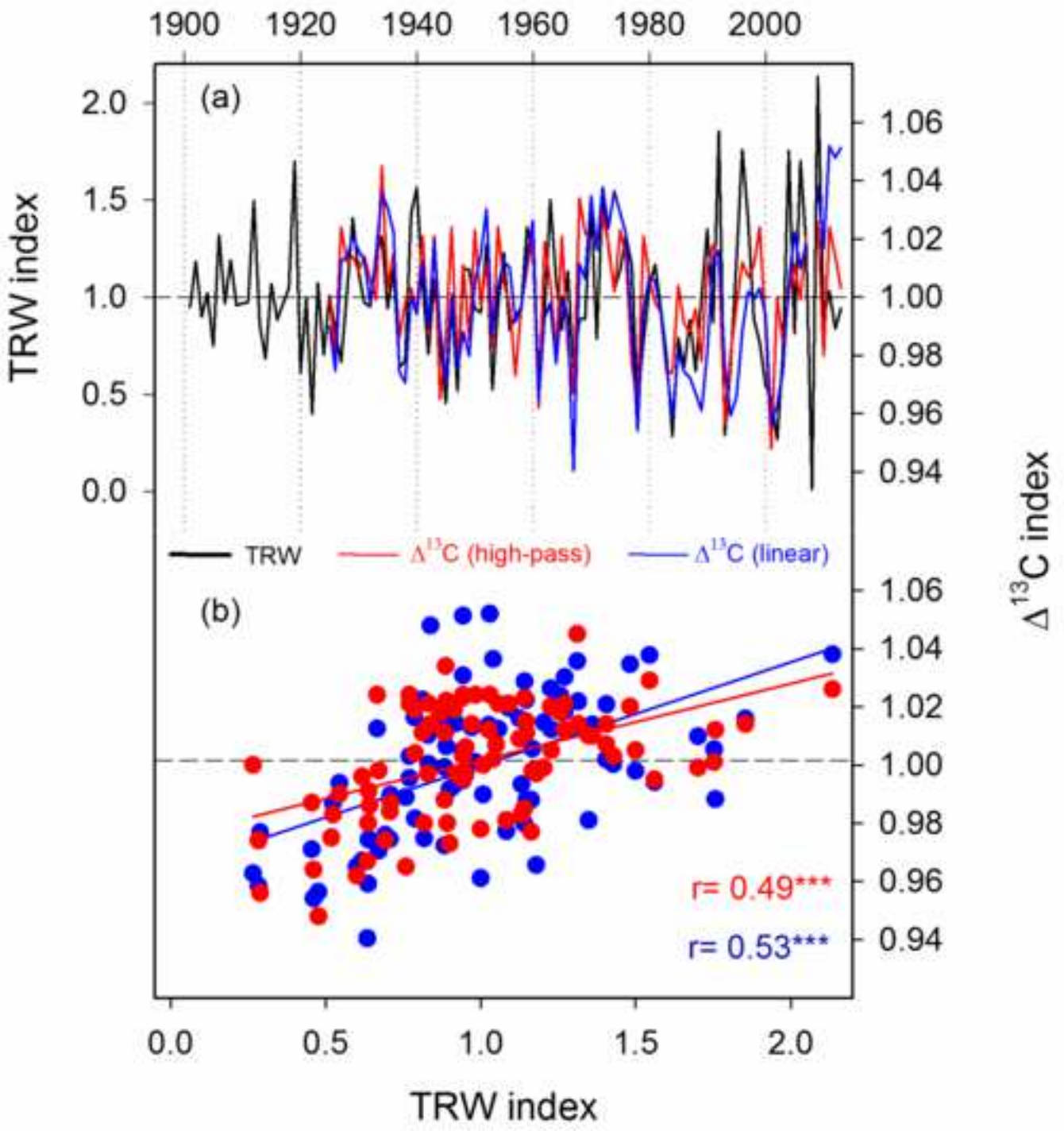

Figure 5

Click here to download Figure Fig5.TIF

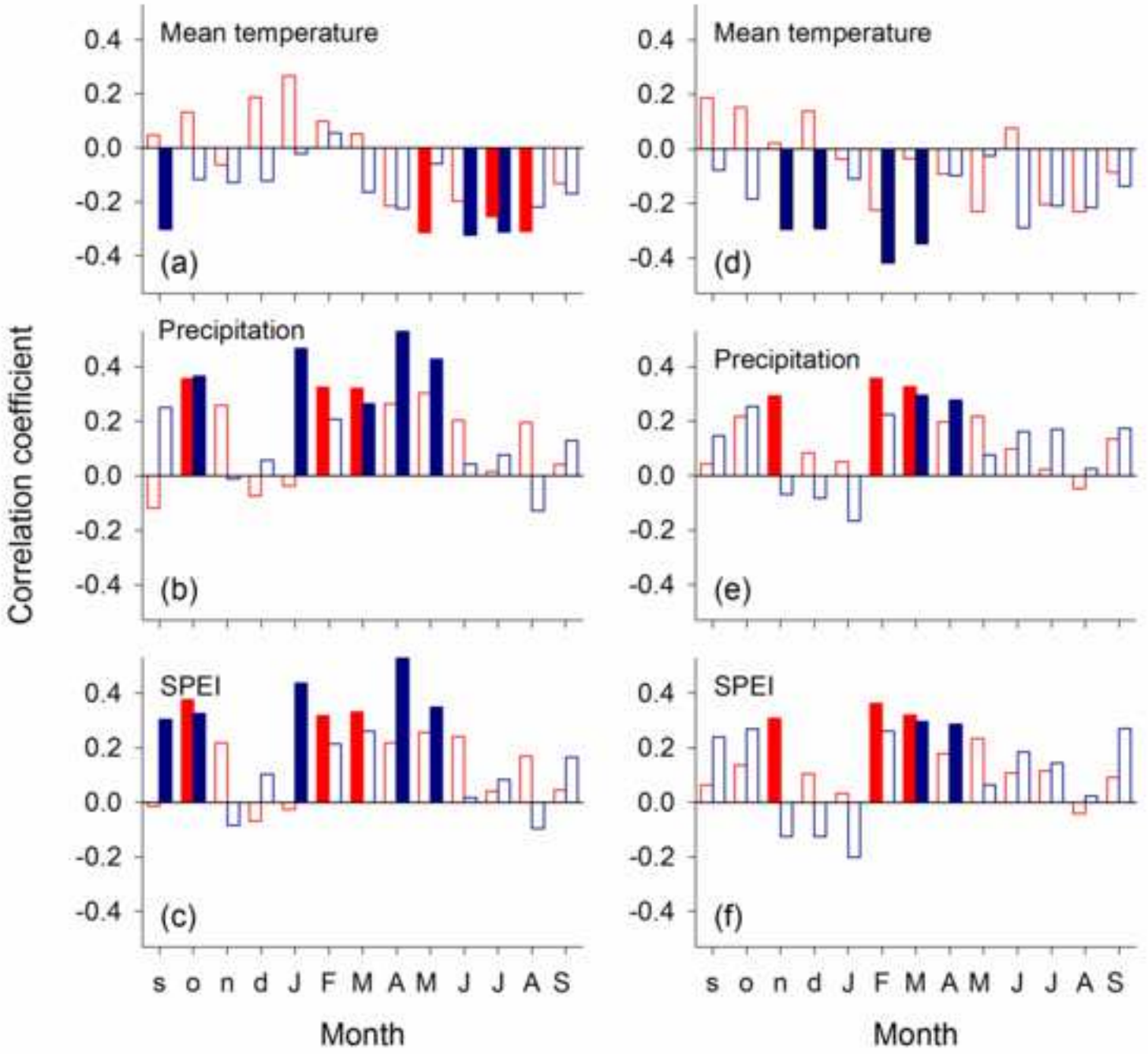

Figure 6

Click here to download Figure Fig6.TIF

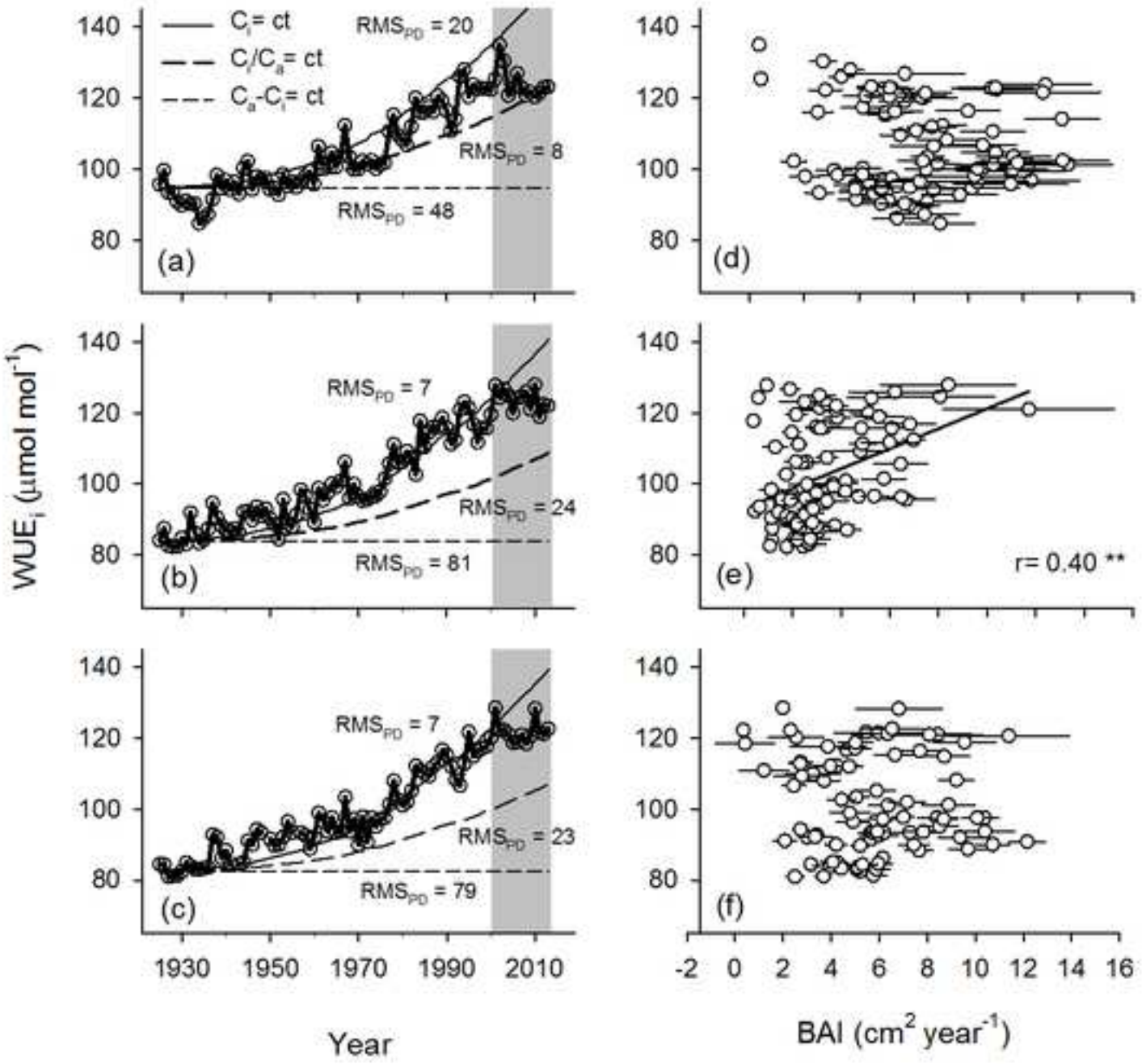

European Journal of Forestry – Electronic Supplementary Material

Quarantining the Sahara desert: Growth and water–use efficiency of Aleppo pine in the Algerian Green Barrier

Zineb Choury[1], Tatiana A. Shestakova[2], Hocine Himrane[3], Ramzi Touchan[4], Dalila Kherchouche[5], J. Julio Camarero[6], Jordi Voltas[1*]

[1]Department of Crop and Forest Sciences – AGROTECNIO Center, University of Lleida, E–25198 Lleida, Spain

[2]Department of Ecology, University of Barcelona, E–08028 Barcelona, Spain

[3]Institute National de Recherche Forestière, Arboretum de Bainem, B.P. 37 Cheraga, Algeria

[4]Laboratory of Tree Ring Research, The University of Arizona, Tucson, AZ 85721, USA

[5]Institute of Veterinary and Agronomy Sciences, The University Hadj-Lakhdar, Batna 05000, Algeria

[6]Pyrenean Institute of Ecology, IPE–CSIC, E–50059 Zaragoza, Spain

*Corresponding Author:

Jordi Voltas

Department of Crop and Forest Sciences – AGROTECNIO Center University of Lleida.

Alcalde Rovira Roure 191, E–25198 Lleida, Spain

tel. +34 973 702855; e–mail: jvoltas@pvcf.udl.cat

CAPTION

This Electronic Supplementary Material contains 5 figures.

Fig. A1 Aleppo pine (*Pinus halepensis*) stands at the natural forest area of Sénalba Chergui, Djelfa province (Saharan Atlas, Algeria). a) North–facing slope, b) and c) Plateau area, and d) South–facing slope of the main ridge of Ouled Naïl mountain (*ca*. 1350 m a.s.l.)

Fig. A2 a) Regional master chronologies for tree–ring width (TRW) (black line, this study; grey line, Tobji, Djelfa region). The Tobji data are taken from Touchan et al. (2011) (data available online at https://www.ncdc.noaa.gov/paleo/study/9920, accessed on April 8th, 2016). TRW records were subjected to high–pass filtering (cubic smoothing spline with a 50% frequency cut–off of 67 years). b) Relationship between the standardized TRW chronologies (*x*-axis, this study; *y*-axis, Tobji, Djelfa region) (***: $P<0.001$)

Fig. A3 Tree–ring width (left panels) and carbon isotope discrimination ($\Delta^{13}C$) (right panels) responses to climate. Relationships with climate are based on bootstrapped correlations between tree–ring indices (obtained by cubic smoothing spline with a 50% frequency cut–off of 100 years for ring–width and by linear detrending for $\Delta^{13}C$) and monthly mean temperature (a, d) , precipitation (b, e) and the Standardized Precipitation Evapotranspiration Index (SPEI) drought index at the 1–month scale (c, f) for the period of 1925–2013. Monthly mean temperatures were linearly detrended to eliminate the effect of the warming trend from the temporal series; therefore, correlations with tree–ring indices were performed using residuals of linear trends. Significant correlation

coefficients (P<0.05) are indicated by filled bars. Lowercase and uppercase letters on the *x*–axes correspond to the years before and during tree–ring formation, respectively

Fig. A4 Soluble sugars (SS), starch and total non–structural carbohydrates (NSC) in sapwood of Aleppo pine (*P. halepensis*) trees growing in a Plateau site, a North slope and a South slope at the natural forest area of Sénalba Chergui, Djelfa province (Saharan Atlas, Algeria). For each carbohydrate component, bars with different letters denote significant differences (P<0.05).

Fig. A5 Combined carbon isotope discrimination ($\Delta^{13}C$) time series of the three study sites for the common period of 1925–2013 (red circles; vertical lines denote standard errors). For comparison, the figure includes (i) a recent $\Delta^{13}C$ chronology from Gúdar, Iberian range (eastern Spain), a site of similar altitude (1,100 m a.s.l.) but higher annual precipitation (465 mm) and lower mean temperature (10.5 °C) than Djelfa (green triangles; Shestakova et al. unpublished) and (ii) a biannual $\Delta^{13}C$ series from Purchena (Almeria province, southeastern Spain; blue squares; Del Castillo et al. 2015), also a high–altitude site (900 m a.s.l.) with slightly higher annual precipitation (376 mm) but higher mean temperature (16.6 °C) compared with Djelfa. The coefficient of determination for each linear trend is included in the figure, but only significant linear trends are plotted.

Figure A1

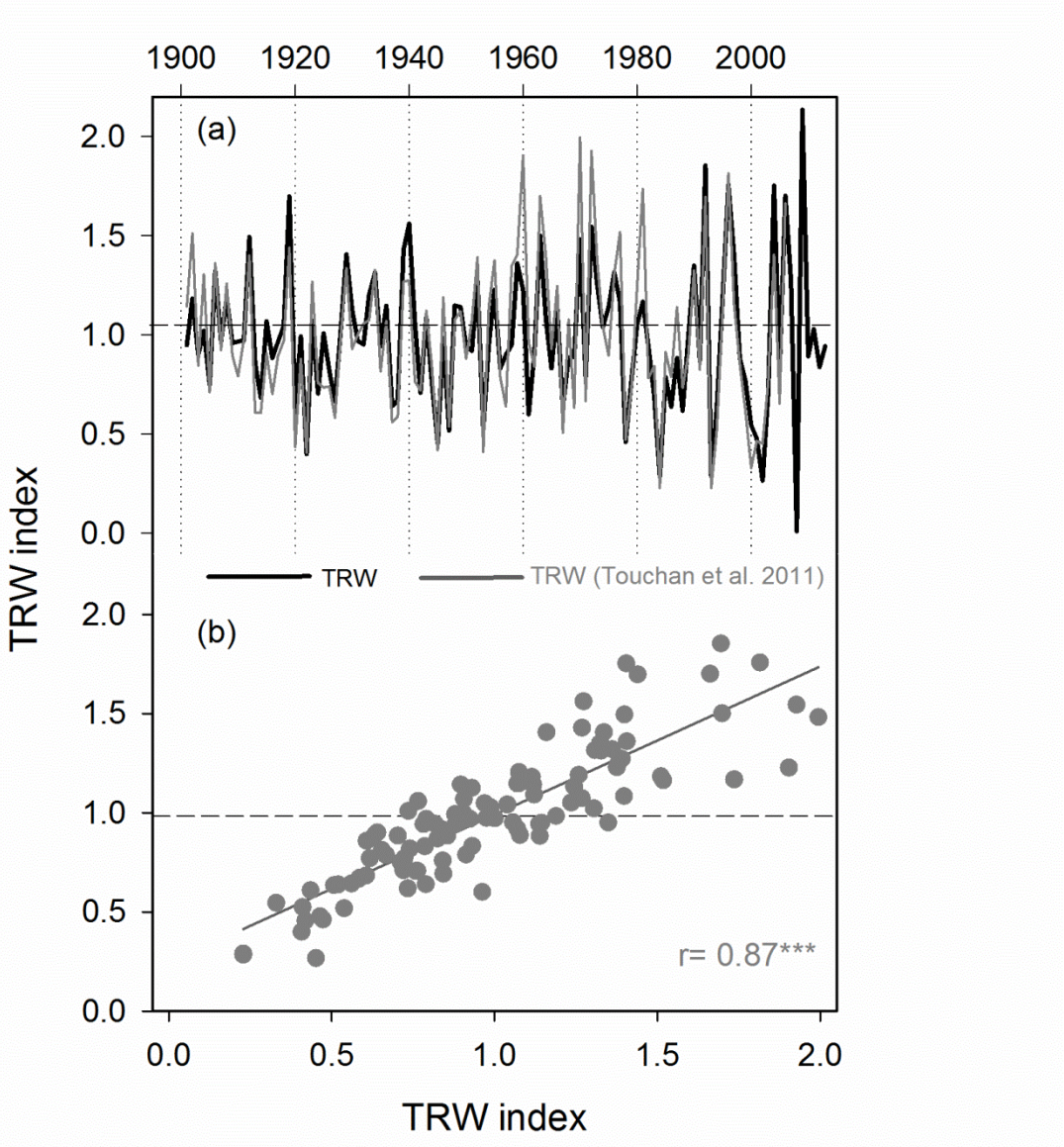
1900
1920
1940
1960
1980
2000
(a)
2.0
1.5
1.0
0.5
0.0
TRW index
TRW
TRW (Touchan et al. 2011)
(b)
2.0
1.5
1.0
0.5
0.0
r= 0.87***
0.0
0.5
1.0
1.5
2.0
TRW index

Figure A2

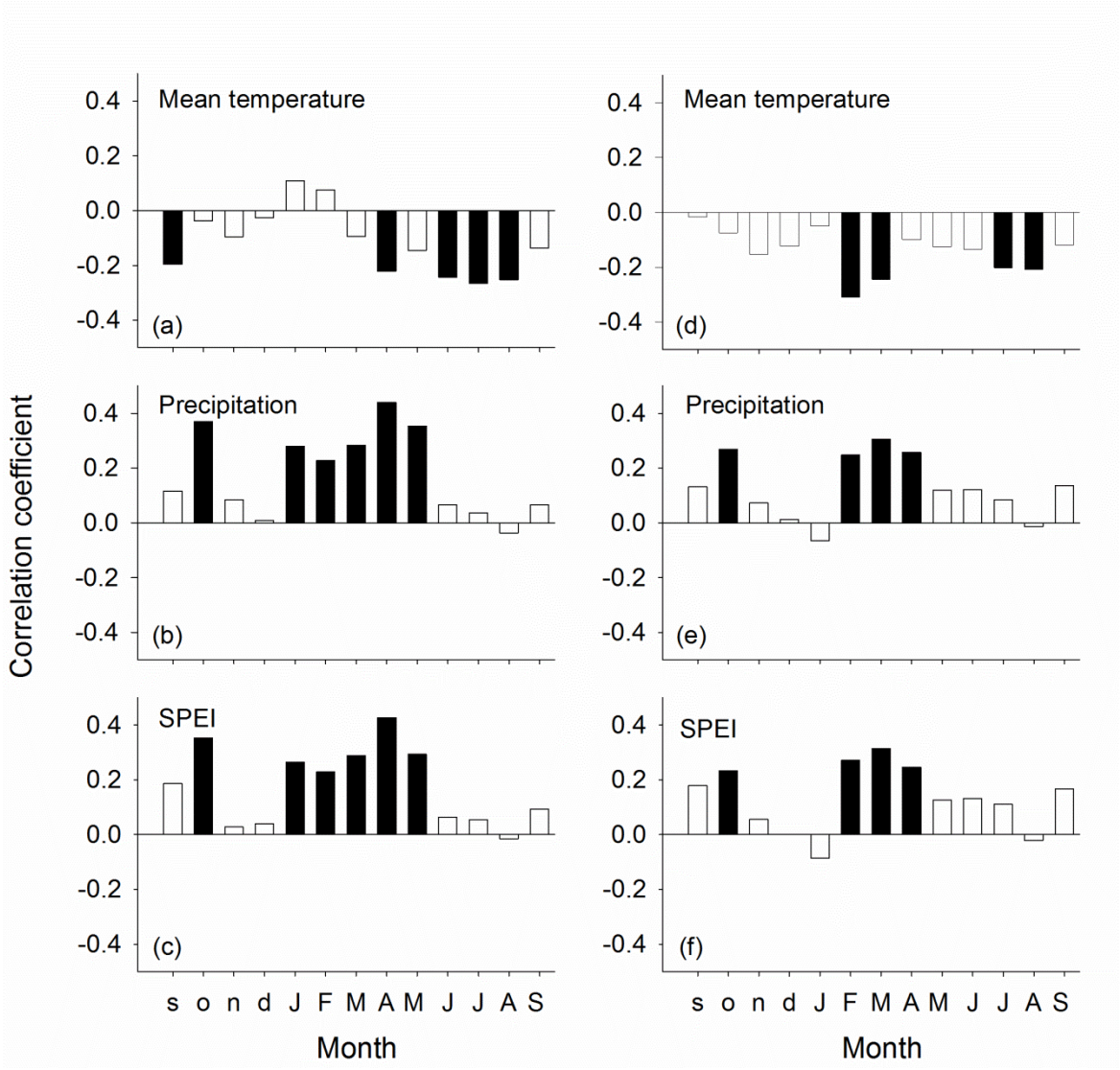
Correlation coefficient
Mean temperature
Precipitation
SPEI
(a)
(b)
(c)
(d)
(e)
(f)
0.4
0.2
0.0
-0.2
-0.4
s o n d J F M A M J J A S
Month

Figure A3

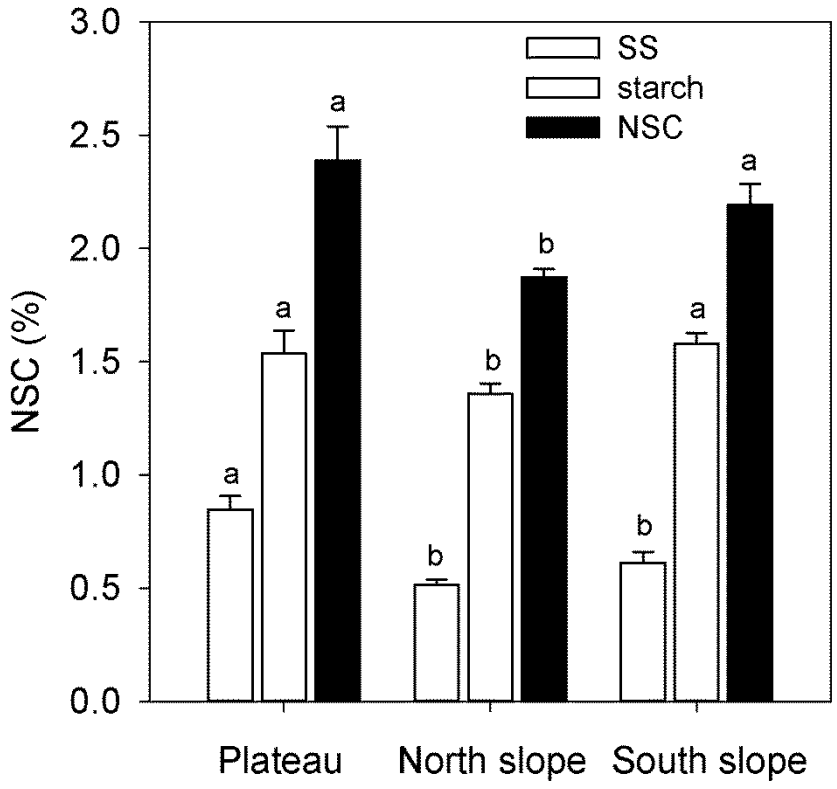
3.0
2.5
2.0
1.5
1.0
0.5
0.0
NSC (%)
SS
starch
NSC
a
a
a
b
b
b
b
a
a
Plateau
North slope
South slope

Figure A4

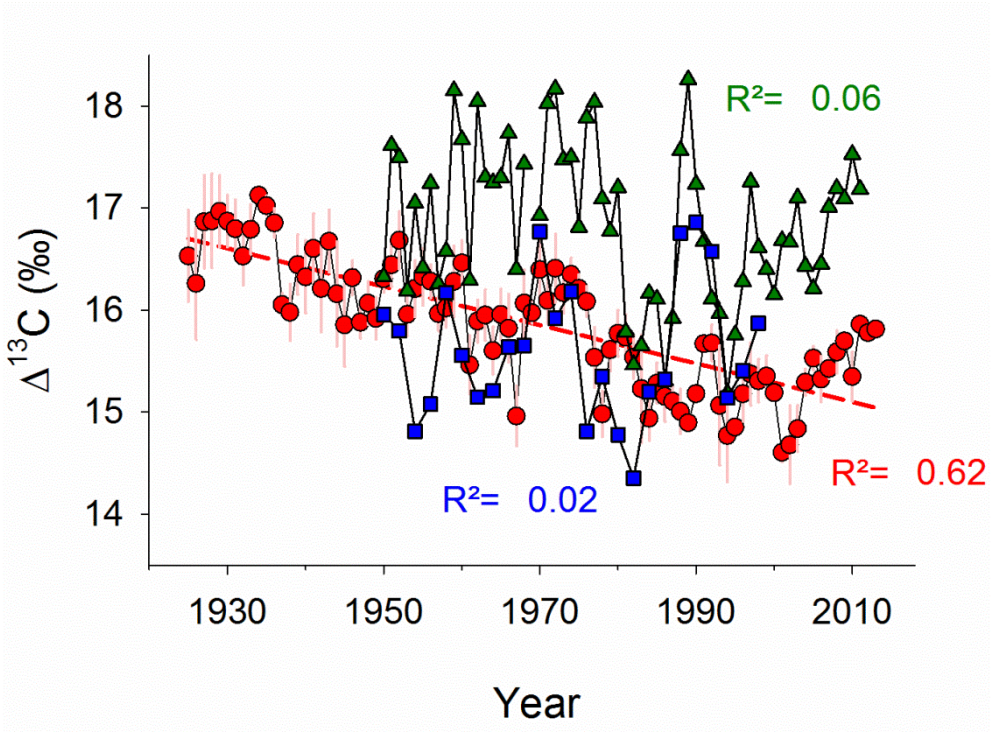
18
17
16
15
14
Δ13C (‰)
1930
1950
1970
1990
2010
Year
R²= 0.06
R²= 0.02
R²= 0.62

Figure A5